

NUCLEON - NUCLEON INTERACTIONS AT SHORT DISTANCES

Misak M. Sargsian *

Florida International University, Miami, Florida, USA

Abstract

Despite the progress made in understanding the NN interactions at long distances based on effective field theories, the understanding of the dynamics of short range NN interactions remains as elusive as ever. One of the most fascinating properties of short range interaction is its repulsive nature which is responsible for the stability of strongly interacting matter. The relevant distances, ≤ 0.5 fm, in this case are such that one expects the onset of quark-gluon degrees of freedom with interaction being dominated by QCD dynamics. We review the current status of the understanding of the QCD dynamics of NN interactions at short distances, highlight outstanding questions and outline the theoretical foundation of QCD description of hard NN processes. We present examples of how the study of the hard elastic NN interaction can reveal the symmetry structure of valence quark component of the nucleon wave function and how the onset of pQCD regime is correlated with the onset of color transparency phenomena in hard pp scattering in the nuclear medium. The discussions show how the new experimental facilities can help to advance the knowledge about the QCD nature of nuclear forces at short distances.

PACS 12.38.-t, 13.75.Cs, 21.30.-x. **Keywords:** Nuclear Forces, QCD, NN Interaction, Hard Processes.

1. Introduction

After the discovery of the Atomic Nuclei in 1911 [1] and the observation of strong nuclear forces in 1919 [2, 3], the understanding of Nuclear Physics on a fundamental level is still an enduring intellectual challenge. We know why atomic nuclei are bound but we don't know why they are stable in the way they are, especially heavy nuclei. The Stability Theorem [4]

*E-mail address: sargsian@fiu.edu

requires a repulsive interaction in order to heavy nuclei not to collapse to the configurations with the radius of ≈ 0.5 fm and per nucleon binding energy of 1500 MeV!

It is remarkable that such a repulsive interaction was eventually found in the short range part of the Nucleon-Nucleon (NN) interaction, when the analysis of the NN scattering data by Jastrow in 1951 [5] unambiguously demonstrated the existence of the repulsive interaction in the NN systems at ≤ 1 fm.

The short-range nature of nuclear forces indicates that the bulk of the dynamics of atomic nuclei can be understood from the dynamics of the NN interaction. Therefore it is not surprising that special emphasis is given to the studies of NN interaction throughout the history of nuclear physics.

If one studies the NN interaction starting from large distances (say ≥ 2 fm), one first observes a clear dominance of the long range one-pion exchange interaction. By decreasing the separation of nucleons to 1.2 – 1.5 fm one will observe the onset of the strong contribution due to two-pion exchange forces resulting in the tensor interaction. The observed magnitude of the tensor as well as strong spin-orbit interactions, however, requires an addition of the vector component to the exchanged forces whose contribution gradually increases with the decrease of NN separations and dominates the overall interaction in the region of the repulsive core at ≤ 0.5 fm. The above picture allows us to identify three main regions (similar to Ref. [6]) for NN interactions which are characterized by their unique dynamics and therefore by their specific theoretical approaches in describing the NN forces.

Long to Intermediate Range: The biggest success in understanding the nuclear forces is achieved in describing long range and long to intermediate range pion exchange interactions based on the effective theories (e.g. [7, 8, 9, 10]). The advantage of these theories is that they satisfy the symmetries of QCD Lagrangian and the interaction vertex is fixed by the mechanism of the Chiral symmetry breaking. Effective theories can be extended to the intermediate-short range distances by introducing contact interactions. Such an approach is successful in describing the intermediate - long range part of the NN interaction, however no dynamical insight can be achieved on the structure of the short-range interaction.

Intermediate to Short Range: Intermediate to short range interactions are currently based fully on phenomenological approaches. In One Boson Exchange Potential (OBEP) models the vector meson exchanges are introduced with phenomenological coupling constants with the assumption that they account for the field theoretical effects of multiple scattering, self interaction of exchanged mesons, etc. (for review see Ref. [11]). The other approach is in phenomenological parameterization of the NN interaction potential in the form of the sum of Yukawa type interactions (e.g. Ref. [12]). In both cases the parameters entering the approximations are fixed by fitting the calculations to the phase shifts of interactions extracted from the analysis of the NN scattering data. In fact the major success of these models are in part due to the significant improvements in quality and quantity of NN phase-shift data by SAID [13, 14] and Nijmegen [15] groups.

Despite the progress in quantitative description of NN interactions up to the lab kinetic energies of 350 MeV the difficulty is however in the fact there is no clear cut constraints that QCD can impose on the dynamics of the interaction in these approaches.

Short Range: Concerning the short range ($< 0.5 - 0.7$ fm) interaction, the most fascinating part of it is the repulsive core which we know is responsible for the stability of atomic nuclei. This is the largely unknown part of the nuclear forces. It is worth mention-

ing that the most modern phenomenological parameterizations [12] of NN potentials still use the Wood-Saxon type function for the repulsive part of the interaction parameterized in 60's. What concerns OBEP models, here the biggest inconsistency is that one considers the exchange of composite particles (bosons) which have sizes comparable to or larger than the internucleon distances being considered. In the language of Feynman diagrams this situation is reflected in the fact that exchanged mesons are highly virtual (their virtuality being comparable with their masses). In this respect it is worth to quote Richard Feynman who noticed that "In fact a "pion far off its mass shell" may be a meaningless - or at least highly complicated idea" [16].

Short Ranges and QCD: The interesting aspect of the short range repulsive interaction is that it operates at distances of ≤ 0.5 fm at which one expects full onset of the QCD degrees of freedom. Therefore our expectation is that the NN interaction should be strongly related to the QCD dynamics at these distances.

The current experimental and theoretical situation in understanding the QCD dynamics of NN interaction at short distances is very incomplete. The available experimental data indicate the rich dynamics at short-range NN interaction. However, no new data were taken since mid 1990's after re-profiling the AGS at Brookhaven National Lab as an injector for Relativistic Heavy Ion Collider as well as completion of the Saturne II project at Saclay [17]. The halt of the flow of experimental data significantly restricted the possibility of further theoretical development. This situation is expected to change in the near future with the advent of high energy hadronic machines at J-PARC (Japan) [19], PANDA (Germany) [20] as well as the currently discussed NICA(Russia) [21] and HIAF(China) [22] projects.

Outline: In this work we review briefly the history of QCD studies of NN interactions (Sec.2.) and highlight the outstanding theoretical and experimental issues in understanding the QCD structure of high energy and momentum transfer (hard) NN interactions (Sec.3.). We then present the theoretical foundation of hard QCD processes relevant to NN interaction (Sections (5.-6.)). First we consider the amplitudes of NN interaction in helicity basis, most appropriate for high energy scattering. Then, anticipating the helicity conservation in the perturbative regime of QCD in Sec.4. we discuss in detail the polarization observables in elastic NN interaction and derive several useful sum rules and equalities for polarization asymmetries that can serve as a tool for identifying the onset of helicity conservation in the hard QCD regime. In Sec.5. we discuss the other signature of the QCD regime of hard NN Scattering - the quark counting rule. Sec. 6. elaborates the light-front dynamics of hard NN scatterings, the definition of light-front wave function of nucleons as well as quark helicity spinors in the light-front, giving us the main theoretical tools for studying hard NN interactions. In Sec. 7. we consider a few examples of the application of the above mentioned theoretical approaches in the quark-interchange model of NN interaction, comparing the results with the limited experimental data currently available. Section 8. summarizes the results and gives some outlook on other possibilities of studying NN systems at short distances.

2. Brief History of QCD approaches to Short Range NN Interaction

The QCD approach in studies of high momentum and energy transfer NN interactions revealed a very rich picture of strong interactions, introducing completely new subjects into the discussion of nuclear forces such as dimensional counting rules, helicity conservations, minimal Fock components, hidden color, etc...

Quark-Gluon Interactions and NN Scattering: First attempts to understand short range properties of NN interaction within QCD were made in the 1970's [23, 24, 25], in which the phenomenology of NN interaction was confronted with the quark-interchange and three gluon exchange mechanisms of hadronic interactions. The real boost in studies of hard hadronic processes in general and NN interaction in particular came after the discovery of dimensional counting rules [26, 27, 28] for fixed large center of mass angle high energy processes. The counting rules gave new observables to explore in hard processes such as the exponents of the energy dependences of scattering cross sections. The most intriguing part of it was that such dependences were naturally predicted within QCD in the picture of hard gluon exchanges between current quarks in hadrons.

The another feature of the processes proceeding through the hard gluon exchanges was the prediction of helicity conservation and new relations between different spin observables in the hard hadronic processes [29, 30]. Naturally, the most accessible hadronic processes were the NN scatterings and there were several dedicated experiments on measuring different spin observables in hard NN processes. However, the experimental results were at best controversial [31, 32] with the most "damaging" being the measurement of the A_{nn} polarization [33, 34], which observed that for 90° center of mass elastic pp scattering at $p_{Lab} = 11.75$ GeV/c, the cross section of protons scattering with parallel spins normal to the scattering plane is four times the one with the antiparallel spins.

The Quark-Gluon Wave Function of the Nucleon: To calculate the NN scattering cross section within QCD, one needs, as an input, the quark-wave function of the nucleon. However, this wave function is poorly known due to the immense complexity of the QCD picture of the nucleon in which the number of quark and gluon constituents are not conserved (for the recent review on bounds rates in QCD see Ref.[35]).

On the other hand, the advantage of high energy and momentum transfer reactions is that they allow a successful application of Fock-component approach to describing the wave function of a nucleon. This approach allows us to start with the minimal Fock component of the nucleon consisting of only three valence quarks and treat the higher order Fock-components as corrections since they are suppressed by additional inverse orders of the invariant momentum transfer.

Concentrating the minimal-Fock component of the nucleon, the next question is what symmetry of valence quarks one needs to consider in the wave function of the nucleon. Here the most natural is to consider the SU(6) symmetry based on the fact that the very same symmetry seems to be realized in constituent quark model which describes the baryonic spectrum reasonably well. Indeed the SU(6) symmetry was one of the the first approaches in describing hard NN processes [29, 30]. Also the constituent quark formalism described reasonably well several properties of intermediate energy NN scattering within the SU(6) symmetry [36].

QCD and Short-Range Structure of the NN-Bound System: The third aspect which is worth to emphasize in relation to studies of NN interaction at short distances is the dynamics of the NN-bound system probed at short distances. The deuteron studies opened up a new realm in studies of QCD dynamics of strong forces. It was realized in Refs. [37, 38, 39, 40, 41], that the fact, that the deuteron is a colorless 6-valence-quark system, creates an additional possibility for existence of color-octet three-quark (3q) states that combine into color-singlet 6-quark combinations (referred as hidden color states). The calculations indicate that there is a substantial hidden color component in the NN bound system at short distances in which the 6q system becomes a relevant degree of freedom.

The notion of the hidden-color component gave a new possible meaning to the NN repulsion which can be in part due to orthogonality between the initial two color octet and final two color singlet nucleons. The other implication of the hidden color component is the prediction of the large contribution from the $\Delta - \Delta$ component in the NN interaction following from the decomposition of the color-singlet 6-quark system.

3. Outstanding Questions of NN Interactions at Short Distances.

There are many unresolved questions which are related to the nucleon-nucleon interactions at short distances with implications ranging from particle physics to astrophysics. With the expectation of a new generation of experimental studies of hard NN processes in the near future, it is worth enumerating several of the problems which can be addressed in the experiments at facilities mentioned earlier (Sec.1.).

Persistence of the Nucleonic Degrees of Freedom: Recent observations of large ($\sim 2M_{Sun}$) neutron star masses [42] indicates existence of rather unreasonably stiff equation of state of the nuclear matter, which is related to the persistence of the nucleonic degrees of freedom [43] at such high densities in which one expects plenty of inelastic transitions and strong overlap of nucleon wave functions. Such persistence is also observed in probing short-range proton-neutron correlations in the nuclei [44, 45] in which the theoretical analysis [46] shows that for up to ≤ 1 fm separations, the NN system has no apparent non-nucleonic component, consisting almost entirely from proton and neutron.

It is interesting that this observation also has its reflection in the modification of partonic distributions of bound nucleons in the nuclear medium (EMC effect). Here, the recent analysis [47] indicates a rather small modification of nucleons in the medium of heavy nuclei, which seems puzzling.

Such a persistence of the nucleons in the high density nuclear environment can be due to the short range repulsion, since the attractive interaction will make the composite system very responsive to medium modifications.

Oscillatory Energy Dependence of the Scaled Cross Section of Hard NN Interaction: Even though the fixed angle high energy NN scattering demonstrated rather unambiguous s^{-10} invariant energy dependence, in agreement with quark counting rules [27, 26, 28], the more careful analysis revealed a violation of this dependence in a rather peculiar form: while the quark-counting rule predicts energy independence of $s^{10} \frac{d\sigma}{dt}$, the data

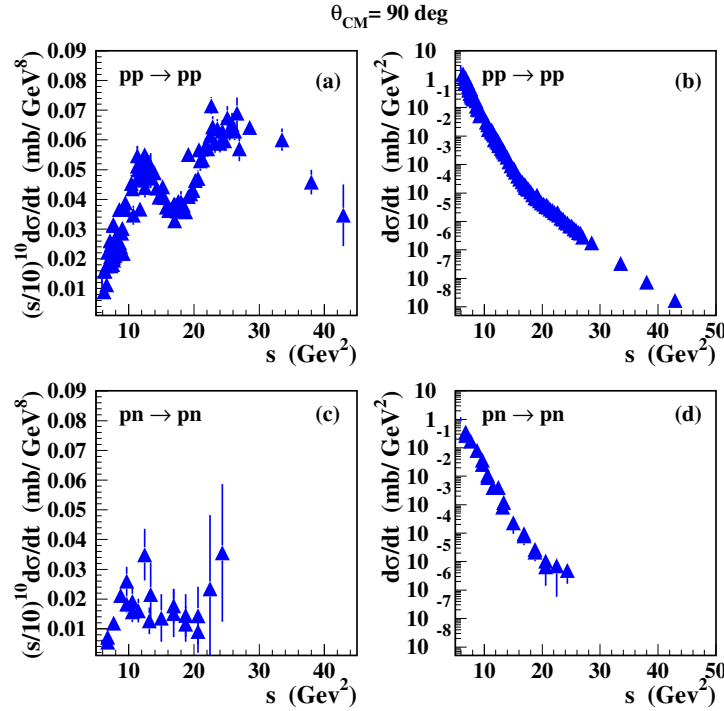


Figure 1. The invariant energy dependence of elastic pp and pn differential cross sections unweighted (b) (d) and weighted by s^{10} factor (a), (c). The experimental data are from Ref. [50, 51, 52, 53, 54].

clearly demonstrate an oscillatory energy dependence of this combination (Fig.1). These regularities observed in this residual energy dependence are striking and despite several intriguing explanations [48, 49], their origin is not understood. In Ref. [48] it is assumed that in addition to the quark-interchange mechanism of hard NN scattering which is sensitive to the quark-gluon interaction at very short distances, the three-gluon exchange mechanism contributes to the overall scattering amplitude. The latter (often referred to as Landshoff mechanism [25]) does not require a quark-interchange, thus, the short distances are not necessarily involved in the NN interaction. Because of the possible Chromo-Coulomb phase shift, the two amplitudes enter with the relative phase that can be tuned to describe the observed energy oscillations.

In Ref. [49] it is assumed that the oscillations are due to the interference of the quark-interchange pQCD amplitudes and the amplitudes of near-threshold s -channel strangeness and charm productions with possible resonating configurations having quantum numbers of $J = 1$, $L = 1$ and $S = 1$. With the relative phases of the pQCD and resonating amplitudes taken as a free parameter, it was possible to describe the observed energy dependences reasonably well.

Overall, in both approximations the assumption is that the pQCD short-range quark-interchange amplitude is interfering with another amplitude which represents a spatially extended system.

Concluding this discussion, it is worth noting that the irregularity in the energy dependence is on a level of 60% in the region where the magnitude of the hard elastic pp cross section changes by *eight* orders of magnitude (Fig.1(b)). As Figs.1(b) and (c) show, the same is apparently true for pn hard elastic scattering.

Anomalous Polarization Asymmetries in Hard NN Scattering: One of the biggest challenges in understanding the QCD dynamics of hard NN interactions came from the observation of large out-of-plane polarization effects at 90° cm scattering for incoming proton momenta as large as $p_{lab} = 11.75$ GeV/c (Fig.2). The surprise in these results is that the experiment found that the elastic cross section of the protons that scatter with their spins parallel and normal to the scattering plane is almost *four* times larger than the cross section when the spins are antiparallel.

The A_{nn} experiment resulted in a flurry of theoretical activity (see e.g. [29, 30, 55, 56, 57, 58, 59, 60, 61]). However the origin of large asymmetry and its energy dependence are still unresolved.

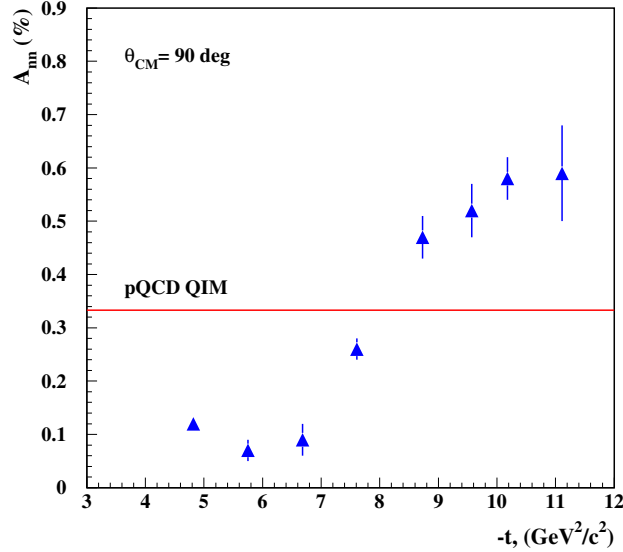


Figure 2. The $-t$ dependence of the analyzing power parameter (A_{nn}) of hard elastic pp scattering. Data are from Ref. [34]. The curve labelled as "pQCD QIM" is the prediction within pQCD quark interchange model (Sec.7).

The implication of this result is that, in order to generate such a large polarization effects, one needs to have a large contribution from the double-spin flip amplitude ϕ_2 or negligible contribution from the helicity conserving ϕ_1 amplitude (see Sec.7.). However, the challenge here is that in the hard QCD regime, the ϕ_2 is the most suppressed and the ϕ_1 is the largest. Another challenge that the experiment posed was (again) the "oscillatory" energy dependence of the asymmetry (Fig.2). Its difference from the basically energy independence of the pQCD quark-interchange prediction is rather striking (Fig.2),

The above situation indicates that, whatever the origin of this large asymmetry is, it is related to the contribution of a spatially extended configuration into the process of the pp scattering. The oscillatory energy dependence indicates that there is an interference between short and long range phenomena. For example, the earlier mentioned charm threshold enhancement effect with the intermediate $J = 1, L = 1, S = 1$ quantum state results in $\phi_1 = 0$ and its interference with the background pQCD QIM process can in principle generate the energy dependence of Fig.2 (see Ref. [49]).

Color Transparency in Hard NN Scattering: One of the most remarkable predictions of QCD is the existence of color transparency phenomena in hard processes taking place in the nuclear environment. The possibility of producing small-sized color-neutral object in hard processes will be evidenced by the reduced absorption of hadrons in propagating through the nuclear medium. The interesting QCD feature is that such a neutral object can be produced both for mesons and baryons. In large momentum transfer, the small distances involved in quark-gluon interaction will require that the quarks in the minimal Fock component of hadron wave function will populate distances $\leq 1/\sqrt{-t}$. Such configurations will have small color dipole moments which will result in reduced strong interaction in the nuclear medium [62, 63]. These expectation resulted in tremendous theoretical and experimental activities in mid 1990's (for review of the subject see e.g. Refs. [64, 65]). The realization that these small-sized configurations are not eigenstates of QCD Hamiltonian of free hadrons and once produced at finite energies they will evolve to normal size hadrons, suggested that the experimental verification of color transparency phenomena is more complex than first expected(see e.g. Ref. [66, 67]).

While the Color Transparency phenomenon or the reduction of the absorption in the nuclear medium is observed for the hard production of $q\bar{q}$ systems [68, 69, 70], the similar effect is still elusive for a qqq system. The first experiments based on the hard $pp \rightarrow pp$ elastic scattering from nuclei [71, 72, 73] demonstrated another "oscillation" feature - this time in the proton beam momentum dependence of the nuclear absorption parameter (Fig.3).

The interesting feature of these data is that initially the transparency grows with the proton momentum above the values expected from Glauber theory, and then after $p_{lab} = 9$ GeV, it falls back leading to transparency values apparently below the Glauber prediction at $p_{Lab} \approx 14$ GeV. The latter indicates that whatever propagates at these energies in the nuclear medium has total cross section larger than that of the NN scattering.

Oscillations Superimposed: If now one superimposes Figs.(1),(2) and (3) recalculating them for invariant energy dependences at given $\theta_{cm} = 90^\circ$ one observes rather interesting correlations between these three different measurements.

First, the data suggest an inverse correlation between the s^{10} weighted pp cross section (Fig.4(a)) and nuclear transparency T_{pp} (Fig.4(c)). This correlation strongly indicates that the broad peak in the pp cross section at $s \approx 25 \text{ GeV}^2$ is related to the spatially large configuration which is strongly absorbed in the nuclear medium as indicated by the drop of the T_{pp} at the same s . Thus, the observed correlation suggests that the nuclei filter the large-size component from the amplitude of hard pp scattering [65]. This picture is reinforced when one compares the s -dependences of the same s^{10} weighted pp cross section (Fig.4(a)) and the polarization asymmetry, A_{nn} (Fig.4(b)). As Fig.4(b) shows, at $s \approx 25 \text{ GeV}^2$ the A_{nn} produces the largest asymmetry well above the pQCD prediction [49] (see Sec.7.),

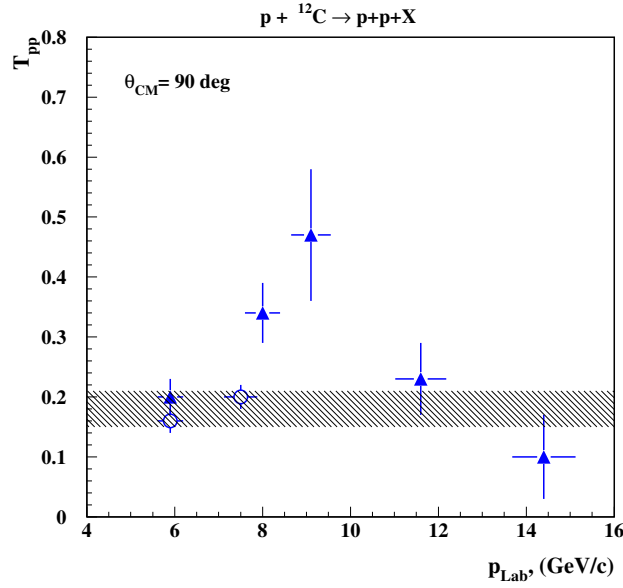


Figure 3. Dependence of the nuclear transparency parameter on the momentum of the incoming proton. Data are from Ref. [72, 73]. Shaded area represents the calculation based on the Glauber theory [74, 75] in which the transparency is defined based on the total cross section of NN scattering.

while the pQCD prediction is closest to the A_{nn} data at $s \sim 18 - 20 \text{ GeV}^2$. The interesting result here is that, at the latter energies ($s \sim 18 - 20 \text{ GeV}^2$) the onset of Color Transparency (less attenuation) is observed in Fig.4(c)). Such a correlation between the agreement of the pQCD prediction of A_{nn} with the data and the increase of the nuclear transparency, T_{pp} , seems to validate the main premise of the Color Transparency prediction, that the small-sized configurations are produced in the pQCD regime which propagate in the nuclear medium with less absorption than ordinary hadrons.

Diquark Signatures of Nucleons: There is a rather rich phenomenology about the quark-diquark structure of the nucleon. This phenomenology follows from the hadron spectroscopy, deep-inelastic scattering, baryon form-factors as well as exclusive hadron interactions (e.g. [76, 77]). The diquark structure reveals itself both as a specific symmetry of quark wave function of the nucleon as well as dynamical component that contributes to the scattering process (for example through the diquark exchange). However, the impossibility of formulation of diquark-structures from the first principles of QCD and its inclusion into the self-consistent evolution equation scheme makes the issue of diquarks an open question in NN scattering physics.

Hidden Color Component in the NN-System: The hidden color component is one of the unique QCD effects in NN interaction that can not be imitated by any baryons degrees of freedom. The hypothesis of the color-neutrality of the observed strongly interacting composite systems introduces the possibilities for a new reality in which baryonic systems

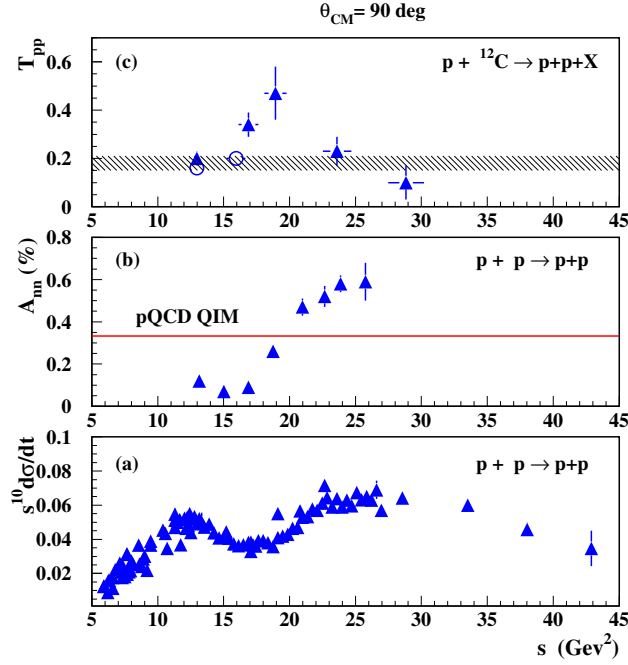


Figure 4. Dependence of the nuclear transparency (c), asymmetry, A_{nn} (b) and s^{10} scaled elastic pp cross section (a) on the invariant energy s .

with high degree of compositeness (one example is NN system) contain explicitly colored three-quark clusters that combine into a color neutral object. One of the best examples is the contribution of two colored baryons, N_c , into the colorless NN system [37, 39, 40]. While existence of such hidden-color components are accepted within QCD there is no clear experimental evidence yet for such components.

4. Helicity Amplitudes and Observables of Elastic NN Scattering

In the following three sections an outline of the theoretical approach is given, which is most suitable for the description of the hard NN scattering in QCD.

The natural framework in describing NN scattering amplitudes at high energies is the helicity description of the quantum states of the nucleon. This representation has the obvious advantage of satisfying the boost invariance of the observable quantities as well as allowing us to define their asymptotic limits in the case of helicity conservation, which is the case in the pQCD regime of the scattering.

For exclusive, $1 + 2 \rightarrow 3 + 4$ scattering of spin-half particles, in general, one has a total of 16 helicity amplitudes $\langle \lambda_3 \lambda_4 | M | \lambda_1 \lambda_2 \rangle$, where λ_i describes the helicity state of the i 'th nucleon having $+\frac{1}{2}$ and $-\frac{1}{2}$ eigenvalues for which we also use the notations $+$ and $-$ respectively¹. Parity conservation and time reversal invariance of strong interaction

¹Subscripts "1", "2", "3" and "4" hereafter represent the incoming, target, scattered and recoil nucleons

as well as the application of generalized Pauli principle (or Isospin symmetry) introduces the following relations between helicity amplitudes of the elastic NN scattering (see e.g. [78, 79]):

$$\begin{aligned}\langle -\lambda_3 - \lambda_4 | M | -\lambda_1 - \lambda_2 \rangle &= (-1)^{(\lambda_1 - \lambda_2 - (\lambda_3 - \lambda_4))} \langle \lambda_3 \lambda_4 | M | \lambda_1 \lambda_2 \rangle \\ \langle \lambda_1 \lambda_2 | M | \lambda_3 \lambda_4 \rangle &= (-1)^{(\lambda_1 - \lambda_2 - (\lambda_3 - \lambda_4))} \langle \lambda_3 \lambda_4 | M | \lambda_1 \lambda_2 \rangle \\ \langle \lambda_4 \lambda_3 | M | \lambda_2 \lambda_1 \rangle &= (-1)^{(\lambda_1 - \lambda_2 - (\lambda_3 - \lambda_4))} \langle \lambda_3 \lambda_4 | M | \lambda_1 \lambda_2 \rangle.\end{aligned}\quad (1)$$

These relations reduce the number of independent elastic NN helicity amplitudes to five which we define as follows:

$$\begin{aligned}\phi_1 &\equiv \langle ++ | M | ++ \rangle = \langle -- | M | -- \rangle \\ \phi_2 &\equiv \langle ++ | M | -- \rangle = \langle -- | M | ++ \rangle \\ \phi_3 &\equiv \langle +- | M | +- \rangle = \langle -+ | M | -+ \rangle \\ \phi_4 &\equiv \langle +- | M | -+ \rangle = \langle -+ | M | +- \rangle \\ \phi_5 &\equiv \langle ++ | M | +- \rangle = \langle -+ | M | -- \rangle = \langle -- | M | +- \rangle = \langle -+ | M | ++ \rangle = \\ &\quad -\langle -- | M | -+ \rangle = -\langle +- | M | ++ \rangle = -\langle ++ | M | -+ \rangle = -\langle +- | M | -- \rangle,\end{aligned}\quad (2)$$

where ϕ_i 's are functions of invariants, s and t , or can be alternately presented as a function of s and the scattering angle, θ_{cm} in the center of mass reference frame. From the above relations it follows that for isotriplet states, particularly for elastic pp scattering at $\theta_{cm} = 90^\circ$, one has $\phi_5^{pp}(\theta_{cm} = 90^\circ) = 0$.

4.1. Practical Observables for Hard Elastic NN Scattering

There is one unpolarized observable which is the cross section of elastic $NN \rightarrow NN$ scattering defined as:

$$\frac{d\sigma}{dt} = \frac{1}{16\pi} \frac{1}{s(s - 4m_N^2)} \sigma_0 \quad \text{with} \quad \sigma_0 = \frac{1}{2}(|\phi_1|^2 + |\phi_2|^2 + |\phi_3|^2 + |\phi_4|^2 + 4|\phi_5|^2) \quad (3)$$

and a total of 256 possible polarization observables in the center of mass reference frame. However, the application of the above mentioned parity conservation, time reversal invariance and generalized Pauli principle reduces this number to 24 independent polarization observables (see e.g. [79]).

Considering the fact that the most of the possible NN scattering experiments in the near future will be performed at fixed-target kinematics, we will consider the polarization observables for the lab frame kinematics. For this purpose we first define the momenta of incoming, target, scattered and recoil nucleons as \mathbf{p}_1 , $\mathbf{p}_2 (= 0)$, \mathbf{p}_3 and \mathbf{p}_4 respectively. Then in addition to three directions defined by above vectors:

$$\hat{\mathbf{p}}_1 = \frac{\mathbf{p}_1}{|\mathbf{p}_1|}, \quad \hat{\mathbf{p}}_3 = \frac{\mathbf{p}_3}{|\mathbf{p}_3|}, \quad \hat{\mathbf{p}}_4 = \frac{\mathbf{p}_4}{|\mathbf{p}_4|} \quad (4)$$

respectively.

one has four following vectors: The one, \mathbf{n} , is transverse to the scattering plane:

$$\mathbf{n} = \frac{\mathbf{p}_1 \times \mathbf{p}_3}{|\mathbf{p}_1 \times \mathbf{p}_3|} \quad (5)$$

and three remaining define in-scattering-plane directions:

$$\mathbf{s}_1 = \frac{\mathbf{n} \times \mathbf{p}_1}{|\mathbf{n} \times \mathbf{p}_1|}, \quad \mathbf{s}_3 = \frac{\mathbf{n} \times \mathbf{p}_3}{|\mathbf{n} \times \mathbf{p}_3|}, \quad \mathbf{s}_4 = \frac{\mathbf{n} \times \mathbf{p}_4}{|\mathbf{n} \times \mathbf{p}_4|}. \quad (6)$$

Based on these directions we define a polarization observable

$$X_{3,4,1,2}, \quad (7)$$

where subscripts 1, 2, 3, 4 correspond to the directions of the polarization of the initial, target, scattered and recoil nucleons. Each of these subscripts can have polarizations along all the above defined directions.

Furthermore, we will present only those polarization asymmetry observables which are experimentally most feasible (or practical) categorizing them by their *degree* of polarization. Also at the right hand side of the each polarization asymmetry observable we give the corresponding expression in the limit of helicity conservation.

Single Polarization:

There is only one nonzero single polarization observable defined by the direction of \mathbf{n} :

$$X_{n,0,0,0} = X_{0,n,0,0} = X_{0,0,n,0} = X_{0,0,0,n} = -\frac{1}{\sigma_0} \text{Im} \left[\phi_5^\dagger (\phi_1 + \phi_2 + \phi_3 - \phi_4) \right] \rightarrow 0. \quad (8)$$

Double Polarizations:

(a) Out-of-plane initial polarization asymmetry and polarization transfer observables:

$$\begin{aligned} X_{0,0,n,n} &= X_{n,n,0,0} = \frac{1}{\sigma_0} \left(\text{Re} \left[\phi_1^\dagger \phi_2 - \phi_3^\dagger \phi_4 \right] + 2|\phi_5|^2 \right) \rightarrow -\frac{1}{\sigma_0} \text{Re} \left[\phi_3^\dagger \phi_4 \right] \\ X_{n,0,n,0} &= X_{0,n,0,n} = \frac{1}{\sigma_0} \left(\text{Re} \left[\phi_1^\dagger \phi_3 - \phi_2^\dagger \phi_4 \right] + 2|\phi_5|^2 \right) \rightarrow \frac{1}{\sigma_0} \text{Re} \left[\phi_1^\dagger \phi_3 \right] \\ X_{0,n,n,0} &= X_{n,0,0,n} = -\frac{1}{\sigma_0} \left(\text{Re} \left[\phi_1^\dagger \phi_4 - \phi_2^\dagger \phi_3 \right] + 2|\phi_5|^2 \right) \rightarrow -\frac{1}{\sigma_0} \text{Re} \left[\phi_1^\dagger \phi_4 \right] \end{aligned} \quad (9)$$

(b) Scattering plane initial state polarization asymmetry observables:

$$\begin{aligned} X_{0,0,s_1,s_1} &= \frac{1}{\sigma_0} \text{Re} \left[\phi_1^\dagger \phi_2 + \phi_3^\dagger \phi_4 \right] \rightarrow \frac{1}{\sigma_0} \text{Re} \left[\phi_3^\dagger \phi_4 \right] \\ X_{0,0,s_1,\hat{p}_1} &= X_{0,0,\hat{p}_1,s_1} = \frac{1}{\sigma_0} \text{Re} \left[\phi_5^\dagger (\phi_1 + \phi_2 - \phi_3 + \phi_4) \right] \rightarrow 0 \\ X_{0,0,\hat{p}_1,\hat{p}_1} &= -\frac{1}{2\sigma_0} \left(|\phi_1|^2 + |\phi_2|^2 - |\phi_3|^2 - |\phi_4|^2 \right) \rightarrow -\frac{1}{2\sigma_0} \left(|\phi_1|^2 - |\phi_3|^2 - |\phi_4|^2 \right) \end{aligned} \quad (10)$$

(c) Helicity transfer and double helicity final state observables:

$$\begin{aligned}
X_{\hat{p}_3,0,\hat{p}_1,0} &= \frac{1}{\sigma_0} \left(-Re \left[\phi_5^\dagger (\phi_1 - \phi_2 + \phi_3 + \phi_4) \right] \sin \theta_3 \right. \\
&\quad \left. + \frac{1}{2} \left[|\phi_1|^2 - |\phi_2|^2 + |\phi_3|^2 - |\phi_4|^2 \right] \cos \theta_3 \right) \rightarrow \frac{1}{2\sigma_0} \left[|\phi_1|^2 + |\phi_3|^2 - |\phi_4|^2 \right] \cos \theta_3 \\
X_{0,\hat{p}_4,\hat{p}_1,0} &= \frac{1}{\sigma_0} \left(-Re \left[\phi_5^\dagger (-\phi_1 + \phi_2 + \phi_3 + \phi_4) \right] \sin \theta_4 \right. \\
&\quad \left. - \frac{1}{2} \left[-|\phi_1|^2 + |\phi_2|^2 + |\phi_3|^2 - |\phi_4|^2 \right] \cos \theta_4 \right) \rightarrow \frac{1}{2\sigma} \left[\phi_1^2 - |\phi_3|^2 + |\phi_4|^2 \right] \cos \theta_4 \\
X_{\hat{p}_3,\hat{p}_4,0,0} &= \frac{1}{\sigma_0} \left(\frac{1}{2} \left[|\phi_1|^2 + |\phi_2|^2 - |\phi_3|^2 - |\phi_4|^2 \right] \cos \theta_3 \cos \theta_4 \right. \\
&\quad \left. + Re \left[\phi_1^\dagger \phi_2 + \phi_3^\dagger \phi_4 \right] \sin \theta_3 \sin \theta_4 - Re \left[\phi_5^\dagger (\phi_1 + \phi_2 - \phi_3 + \phi_4) \right] \sin(\theta_3 - \theta_4) \right) \\
&\rightarrow \frac{1}{\sigma_0} \left(\frac{1}{2} \left[|\phi_1|^2 - |\phi_3|^2 - |\phi_4|^2 \right] \cos \theta_3 \cos \theta_4 + Re \left[\phi_3^\dagger \phi_4 \right] \sin \theta_3 \sin \theta_4 \right), \tag{11}
\end{aligned}$$

where θ_3 and θ_4 are the lab scattering angles of scattered "3" and recoil "4" nucleons.

Triple Polarizations: Here we consider the situations in which the transverse polarization of only one of the final nucleons are measured in addition to the polarizations of initial nucleons:

$$\begin{aligned}
X_{n,0,s_1,s_1} &= X_{0,n,s_1,s_1} = -X_{n,0,\hat{p}_1,\hat{p}_1} = -X_{0,n,\hat{p}_1,\hat{p}_1} = \\
&= -\frac{1}{\sigma_0} Im \left[\phi_5^\dagger (\phi_1 + \phi_2 - \phi_3 + \phi_4) \right] \rightarrow 0 \\
X_{n,0,\hat{p}_1,s_1} &= X_{0,n,\hat{p}_1,s_1} = \frac{1}{\sigma_0} Im \left[\phi_1^\dagger \phi_4 - \phi_2^\dagger \phi_3 \right] \rightarrow 0 \\
X_{n,0,s_1,\hat{p}_1} &= X_{0,n,s_1,\hat{p}_1} = -\frac{1}{\sigma_0} Im \left[\phi_1^\dagger \phi_3 - \phi_2^\dagger \phi_4 \right] \rightarrow 0 \tag{12}
\end{aligned}$$

4.2. Sum Rules and Equalities for Scattering of Identical Particles

The polarization asymmetry observables, defined above, allow us to extract all the individual helicity amplitudes of NN elastic scattering. In practice it is less likely that all of these observables will be experimentally available at some point. However, several sum rules and equalities between different observables (which have better chance of being experimentally measured) will allow us to ascertain the extent of the polarization in the hard scattering regime.

First, it is worth emphasizing that, without invoking the assumption of helicity conservation, for identical particles one can demonstrate the existence of large asymmetries for initial state polarizations at any given high energy scattering at $\theta_{cm} = 90^\circ$. For this, one observes that for identical particles at $\theta_{cm} = 90^\circ$ elastic scattering, (i.e. $pp \rightarrow pp$ scattering) due to the generalized Pauli principle, the amplitudes with a single helicity flip are zero ($\phi_5 = 0$). From the same principle it follows that $\phi_4(\theta_{cm} = 90^\circ) = -\phi_3(\theta_{cm} = 90^\circ)$.

These properties of helicity amplitudes allow us to derive the following relations between the above defined polarization observables at $\theta_{cm} = 90^0$ elastic scattering of protons: The first relation is for double polarized initial states [29, 30]:

$$X_{0,0,n,n}^{pp} - X_{0,0,s_1,s_1}^{pp} - X_{0,0,\hat{p}_1,\hat{p}_1}^{pp} = 1, \quad (13)$$

where for these polarization observables in the literature often the following notations are used: $A_{nn} \equiv X_{0,0,n,n}$, $A_{ss} \equiv X_{0,0,s_1,s_1}$ and $A_{ll} \equiv X_{0,0,\hat{p}_1,\hat{p}_1}$.

The second relation is for the out-of-plane polarization and helicity transfer scatterings:

$$\begin{aligned} X_{n,0,n,0}^{pp} &= X_{0,n,n,0}^{pp} = \frac{1}{\sigma_0} \text{Re} \left[\phi_1^{pp,\dagger} \phi_3^{pp} - \phi_2^{pp,\dagger} \phi_4^{pp} \right] \\ X_{\hat{p}_3,0,\hat{p}_1,0}^{pp} &= X_{0,\hat{p}_4,\hat{p}_1,0}^{pp} = \frac{1}{2\sigma_0} \left(|\phi_1^{pp}|^2 - |\phi_2^{pp}|^2 \right) \cos \theta_3, \end{aligned} \quad (14)$$

where $\theta_3 = \theta_4$ for $\theta_{cm} = 90^0$.

And the third relation is for the triple polarization case:

$$X_{n,0,\hat{p}_1,s_1}^{pp} = X_{n,0,s_1,\hat{p}_1}^{pp} = \frac{1}{\sigma_0} \text{Im} \left[\phi_1^\dagger \phi_4 - \phi_2^\dagger \phi_3 \right]. \quad (15)$$

It follows from Eqs.(13) and (14) that the polarization correlations do not vanish with an increase of energy and they could be quite large. For Eq.(14) the large polarization follows from the expected dominance of the real parts of the amplitudes and observed hierarchy [61] in the hard scattering regime (for any large and fixed θ_{cm}):

$$|\phi_1| \geq |\phi_3| \sim |\phi_4| \gg |\phi_5| \gg |\phi_2|. \quad (16)$$

4.3. Signatures of Helicity Conservation

The onset of the helicity conservation in QCD is associated with the two following properties of helicity amplitudes: *first* the relation of Eq.(16) is established with ϕ_5 and ϕ_2 being negligible and *second* the amplitudes are predominantly real.

For the particular case of the elastic pp scattering at $\theta_{cm} = 90^0$ the onset of the helicity conservation will result in the following relations between double initial state polarization asymmetries:

$$X_{0,0,n,n}^{pp} \approx -X_{0,0,s_1,s_1}^{pp} \approx \frac{1 + X_{0,0,\hat{p}_1,\hat{p}_1}^{pp}}{2} \approx |\phi_3^{pp}|^2 = |\phi_4^{pp}|^2 \quad (17)$$

and most interestingly between initial state polarizations and helicity transfer asymmetries:

$$X_{0,0,n,n}^{pp} - X_{0,0,\hat{p}_1,\hat{p}_1}^{pp} \approx -(X_{0,0,s_1,s_1}^{pp} + X_{0,0,\hat{p}_1,\hat{p}_1}^{pp}) \approx \frac{X_{\hat{p}_3,0,\hat{p}_1,0}^{pp} + X_{0,\hat{p}_4,\hat{p}_1,0}^{pp}}{2 \cos \theta_3} \approx \frac{|\phi_1^{pp}|^2}{2}. \quad (18)$$

For the more general case of hard elastic NN scattering in the helicity conservation regime at large and fixed $\theta_{cm} \sim 90^0$ a rather non-trivial relation exists:

$$X_{\hat{p}_3,0,\hat{p}_1,0} \rightarrow -X_{0,0,\hat{p}_1,\hat{p}_1} \quad (19)$$

which indicates that the helicity transfer asymmetry approaches to the asymmetry of double initial helicity scattering.

For all other observables in the helicity conservation regime one obtains expressions which are given in the RHS parts of Eqs.(8,9,10,11,12). It is worth mentioning that the measurement of the triple-polarizations in Eq.(12) are important for verifying that the helicity amplitudes become real, especially in relation to ϕ_1 , ϕ_3 and ϕ_4 amplitudes.

5. Quark Counting Rules of QCD

About 40 years ago in two seminal papers [26, 27], predictions were made that at fixed θ_{cm} the high energy hadronic processes probe the constituents of hadrons in their minimal Fock component states. This observation stimulated extensive research on hard exclusive hadronic processes.

Within automodelism (scale invariance) assumption the invariant energy dependence of the Feynman amplitude, $|\langle cd | M | ab \rangle|^2$, of hard exclusive $a + b \rightarrow c + d$ scattering is such that it compensates the combined dimensionality of the Fock states of participating hadrons, $[N_a N_b N_c N_d]^{\frac{1}{2}} = m^{n_a+n_b+n_c+n_d-4}$, where N_j 's are the normalization factors and n_j 's are the number of constituents of the Fock component of the j hadron:

$$|j\rangle = N_j^{\frac{1}{2}} |n_j, \text{constituents}\rangle. \quad (20)$$

This results in the simple relation for the energy dependence of the differential cross sections of hard exclusive reactions:

$$\frac{d\sigma^{ab \rightarrow cd}}{dt} = F(\theta_{cm})_{ab \rightarrow cd} s^{-(n_a+n_b+n_c+n_d-2)}, \quad (21)$$

where $F(\theta_{cm})_{ab \rightarrow cd}$ is a function of θ_{cm} only.

As it was observed in Refs. [80, 81] the automodelism assumption is justified for local field theories with vector interaction and thus it could be extended to electromagnetic processes in which case leptons and bare photons would be counted as a one unit of constituent.

One of the most beautiful observations was [27, 28] that the energy counting rule naturally follows from perturbative QCD in which the gluon exchange between massless quarks will provide the scale invariance of the scattering amplitude. Within pQCD one can prove the two main asymptotic rules presented in Fig.5: (a) the sub-process of hard elastic *quark* – *quark* interaction is energy independent (depends only on the scattering angle) and (b) each energetic propagator of intermediate quark line enters with factor, $\frac{1}{s}$. These two rules in addition to the above mentioned counting of leptons and bare photons define all the necessary rules for estimating the energy dependence of differential cross sections of hard exclusive scattering of hadrons, leptons as well as photons in the fixed θ_{cm} kinematics in the $s \rightarrow \infty$ limit.

The important consequence of quark-counting rules is that it explains why one should expect the dominance of the minimal-Fock component in the wave function of the interacting hadrons. The simple estimate shows that higher order Fock components will result in larger negative exponent in the s -dependence of the scattering amplitude and therefore will decrease much faster than the contribution due to minimal-Fock component in the high energy limit.

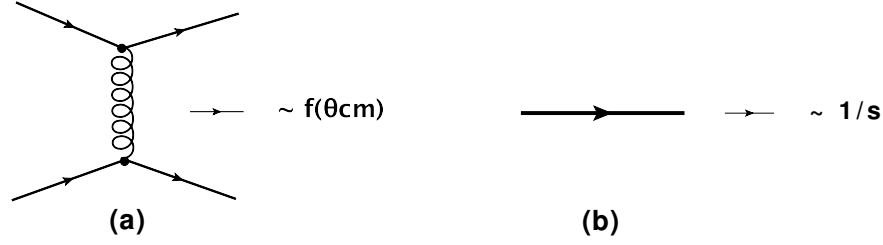


Figure 5. Quark counting rules.

6. Basics of Light-Front Dynamics in QCD

Bound State Problem: One of the fundamental problems in field theory is the description of the quantum bound states in a relativistically invariant form. The problem inevitably arises with the proper treatment of the time at which the bound state is observed as well as the unambiguous identification of the compositeness of a bound state due to the non-trivial structure of the vacuum in field theories. The latter is related to the differentiation of the constituents of the bound system from the particles arising from the vacuum fluctuations.

The problem of the treatment of the time in the relativistic dynamics of the bound states can be seen in the following consideration of the wave function of the system consisting of n particles. To "measure" the wave function of the system, the observer X in Fig.6 (a) must instantaneously measure the positions and times of all n particles. In nonrelativistic dynamics due to Galilean relativity, the n positions can be measured instantaneously at the given absolute time t , allowing one to talk about the wave function of the system defined as $\Psi(z_1, z_2, z_3, \dots, z_n, t)$.

In the relativistic case, the measurement will assume sending light signals from the position of the observer X (Fig.6 (a)) to all n particles resulting in the measurement of the function $\Psi(z_1, t_1, z_2, t_2, z_3, t_3, \dots, z_n, t_n)$. Even if the latter function can be arranged to be relativistically invariant it does not have a meaning of the bound state of the system at the given time, t .

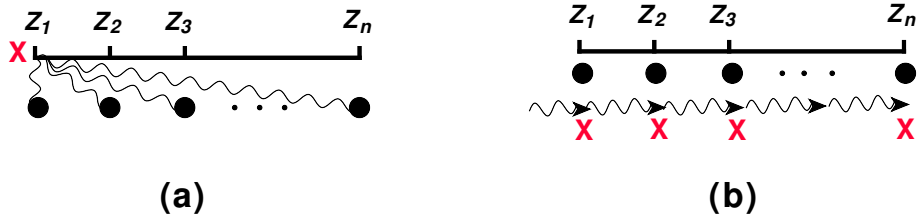


Figure 6. Relativistic measurement of the wave function.

This problem can be solved if the observer "rides" on the front of the light beam that passes through the all n particles. In this case the observer will find that all constituents are measured at the same "light front" time $\tau = t_1 - z_1 = t_2 - z_2 = t_3 - z_3 \dots t_n - z_n$ and can reconstruct the wave function of the system with constituents being measured at light-cone positions of $Z_i = t_i - z_i$, $i = 1, \dots, n$ at the same light-cone time τ : $\Psi_{LF}(Z_1, Z_2, Z_3, \dots, Z_n, \tau)$.

That the relativistic dynamics simplifies in the light-front due to the maximum number of kinematic generators of the Lorentz group, was first observed by P. A. M. Dirac [82]. In relation to relativistic bound states, S. Weinberg [83] demonstrated how the simple structure of the vacuum allows the separation of the constituent structure of the bound state from the vacuum fluctuation contributions.

The light-front dynamics is a natural approach in QCD, in which due to light masses of quarks, one naturally deals with relativistic bound states [84]. In this case, choosing quantization axis by the direction of the momentum of the hadron, its wave function is quantized at fixed $z^+ = t + z$ time with p^- component representing the light-front energy of the hadron. In this approach the Weinberg type equation specifies the quark-gluon wave function of the hadron which depends on the transverse momenta $\mathbf{k}_{\perp,i}$ and the light-front longitudinal momentum fractions (defined as $x_i \equiv \frac{k_i^+}{p^+}$) of the constituent quarks and gluons. The wave function defined in such way is a Lorentz boost invariant and addresses the main issues of the description of the relativistic bound states - Lorentz invariance and definite light-cone time of the quantization.

In practical applications, the quark-gluon wave function of hadrons is expanded into the Fock component representations that allows to account fully the compositeness of the hadrons as a bound system of quarks. For example the Fock-state expansion of the light cone wave function of the nucleon can be presented as [85, 86]

$$\begin{aligned} |\Psi_N^{Sz}(P^+, \mathbf{P}_\perp)\rangle &= \sum_n \prod_{i=1}^n \frac{dx_i d^2 k_{\perp,i}}{\sqrt{x_i} 16\pi^3} (2\pi)^3 2\delta(1 - \sum_{j=1}^n x_j) \delta^{(2)}(\sum_j \mathbf{k}_{\perp,j}) \\ &\times \psi_{n/N}(x_i, \mathbf{k}_{\perp,i}, \lambda_i) |n; x_i p^+, x_i \mathbf{P}_\perp + \mathbf{k}_{\perp,i}, \lambda_i\rangle \end{aligned} \quad (22)$$

where $|n; x_i p^+, x_i \mathbf{P}_\perp + \mathbf{k}_{\perp,i}, \lambda_i\rangle$ represents the eigenstates of Fock-components with n constituents. The coefficients: $\psi_{n/N}(x_i, \mathbf{k}_{\perp,i}, \lambda_i)$ are the probability amplitudes (wave functions) for given n constituents with relative transverse momenta, $\mathbf{k}_{\perp,i}$ and "longitudinal" momentum fractions x_i .

Hard pQCD Interaction in the Light-Front: Using the light cone - helicity spinors in the form [87]:

$$u_\lambda(p^+, p_t) = (p^+ + \beta m + \alpha_t \cdot p_t) \chi_\lambda, \quad (23)$$

where

$$\chi_{\pm\frac{1}{2}} = \frac{1}{\sqrt{2}}(1 + \alpha_3)\chi_\pm, \quad \text{with} \quad \chi_+ = \begin{pmatrix} 1 \\ 0 \\ 0 \\ 0 \end{pmatrix} \quad \text{and} \quad \chi_- = \begin{pmatrix} 0 \\ 1 \\ 0 \\ 0 \end{pmatrix}, \quad (24)$$

for the fermion-vector field vertex one obtains:

$$\begin{aligned} \bar{u}_{\lambda'}(p') \gamma^+ u_\lambda(p) &= 2\sqrt{p'_+ p_+} \delta^{\lambda, \lambda'} \\ \bar{u}_{\lambda'}(p') \gamma^- u_\lambda(p) &= \frac{1}{\sqrt{p'_+ p_+}} \left[(1 + S_{\lambda, \lambda'}) p_R p'_L + (1 - S_{\lambda, \lambda'}) p_L p'_R + m^2 \right] \delta^{\lambda, \lambda'} \end{aligned}$$

$$\begin{aligned}
& + \frac{\Delta_{\lambda,\lambda'} m}{\sqrt{p'_+ p_+}} [(p_R - p'_R)(1 + \Delta_{\lambda,\lambda'}) + (p_L - p'_L)(1 - \Delta_{\lambda,\lambda'})] \\
\bar{u}_{\lambda'}(p') \gamma^{R/L} u_{\lambda}(p) & = \left[\sqrt{\frac{p_+}{p'_+}} p'_{R/L} (1 \mp S_{\lambda\lambda'}) + \sqrt{\frac{p'_+}{p_+}} p_{R/L} (1 \pm S_{\lambda\lambda'}) \right] \delta^{\lambda,\lambda'} \\
& + m \Delta_{\lambda,\lambda'} \left[\sqrt{\frac{p_+}{p'_+}} - \sqrt{\frac{p'_+}{p_+}} \right] (1 - \Delta_{\lambda,\lambda'}), \tag{25}
\end{aligned}$$

where "R" and "L" indices of the given vector A correspond to $A_{R/L} = A_x \pm iA_y$. Also, $S_{\lambda,\lambda'} \equiv \lambda + \lambda'$ and $\Delta_{\lambda,\lambda'} \equiv \lambda - \lambda'$.

By using the light cone gauge for the exchanged gluon propagators, one avoids the necessity of inclusion of the ghost fields to cancel the nonphysical contributions of gluonic fields and, for the interaction "cell" of Fig.5(a) one obtains:

$$\bar{u} \gamma^\mu u d_{\mu\nu} \bar{u} \gamma^\nu u = \bar{u} \left[\frac{\gamma^+}{r^+} r_\perp - \gamma_\perp \right] u \bar{u} \left[\frac{\gamma^+}{r^+} r_\perp - \gamma_\perp \right] u, \tag{26}$$

where r is the four-momentum of the exchanged gluon.

Applying the above defined vertex rules, it is now easy to show, (a) the validity of counting rules of Fig.5 in perturbative QCD and (b) that the counting rules are accompanied by the helicity conservation of interacting quarks. Thus the signature of the quark-counting rules together with the helicity conservation will represent a powerful indicator for the onset of the pQCD regime in strong interactions.

6.1. Non-Perturbative QCD Contribution and Factorization Properties of Hard Scattering Amplitudes

Even though in probing short distance properties of NN interaction our focus is on the pQCD aspects of hard quark-gluon interactions, we cannot avoid the non-perturbative contributions. The latter will appear prominently in the wave functions of nucleons. The necessary assumption that allows us to proceed with the calculation of hard NN scattering amplitudes is the assumption of the factorization of nonperturbative and perturbative QCD contributions [87]. This assumption is based on the very plausible expectation that the dominant contribution from the wave functions of incoming and outgoing nucleons come from the collinear states of their minimal Fock components. In this case, each three quarks of initial nucleon "arrive" at hard scattering "point" with momenta almost parallel to their parent nucleons and after the hard scattering they emerge parallel to the respective momenta of outgoing nucleons. Clearly the wave functions of nucleons containing almost collinear quarks are dominated by the nonperturbative QCD contribution.

Even if such factorization is well justified and applied, another problem is the number of possible diagrams (which is in the order of tens of thousands) which take into account all possible combinations of five hard gluon exchanges between incoming and outgoing collinear quarks. This and the issue of nonperturbative wave functions can be addressed if the calculated quantities are expressed through the experimentally measured quantities such as nucleon-form factors [88] or if we consider the observables such as cross section ratios,

polarization and angular distribution asymmetries which are not sensitive to the absolute normalization of the amplitudes and are sensitive either to the structure of hard scattering or symmetry of the nucleon wave functions.

Below we will consider a few examples in which the above approach is applied in describing the ratios of the hard elastic pn and pp scatterings as well as the angular asymmetry of the hard $pn \rightarrow pn$ scattering around $\theta_{cm} = 90^\circ$.

7. Quark Interchange Mechanism of Hard Elastic NN Scattering

As it follows from Eq.(21), the quark counting rule applied to the hard elastic NN scattering predicts

$$\frac{d\sigma}{dt} = F(\theta_{cm})_{NN \rightarrow NN} \cdot s^{-10}, \quad (27)$$

which, as it follows from the discussion of Sec.3., describes the bulk of the energy dependence of hard NN scattering at large θ_{cm} . According to the application of the quark counting rules, the s^{-10} energy dependence requires the hard exchange of five gluons between six quarks representing the minimal Fock components of two nucleons. One such mechanism that satisfies the above requirement is the quark-interchange mechanism of the NN interactions.

7.1. Dominance of Quark-Interchange Diagrams

Considering the topology of hard QCD scatterings in elastic NN processes one can identify a few possibilities in which the collinear quarks from minimal Fock components of the nucleon wave function can scatter into the final state (Fig.7). In fact the mechanism of independent three-gluon exchanges (Landshoff mechanism [25]) (Fig.7 (c) predicts softer (s^{-8}) energy dependence since it requires less number of gluon exchanges. However this diagram (as well as the one in Fig.7(b)) does not exchange quarks and will contribute equally to NN and $\bar{N}N$ scattering. Thus, comparison of the experimental data of these two reactions will allow the estimation of the contributions of such diagrams. Such a comparison was made in the experiment of Ref. [89] which found the upper limit of the ratio of elastic differential cross sections of $\bar{p}p$ to pp at $p_{Lab} = 9.9$ GeV/c at $\theta_{cm} = 90^\circ$ to be less than 4%. The measurement of the same ratio at $p_{Lab} = 5.9$ GeV/c yielded $\sim 2.5\%$. These results, together with the comparison of the cross sections of twenty different hard exclusive hadronic reactions unambiguously confirmed the dominance of the hard scattering amplitudes of hadrons containing quarks of the same flavor with respect to the scattering amplitudes of hadrons that share no common flavors of quarks.

Thus, one can start with a rather solid experimental justification of the dominance of the quark-interchange (QIM) diagrams of Fig.7(a) in the hard elastic NN scattering amplitude. In fact the theoretical analysis demonstrates that the QIM diagrams represent the dominant mechanism of hard elastic scattering for up to ISR energies (see discussion in [30]). It is worth mentioning that the quark-interchange mechanism also describes reasonably well the 90 c.m. hard break-up of two nucleons from the deuteron [90, 91, 92, 93] and 3He [94].

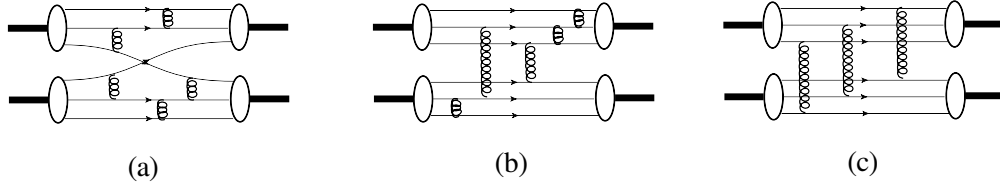


Figure 7. Possible scattering diagrams for elastic NN processes.

Based on the above arguments we now focus on the quark-interchange diagrams which contain five gluon exchanges as shown in Fig.8. Furthermore, we assume the validity of earlier discussed factorization of the minimal (3q) Fock components of initial and final state wave functions of nucleons and the hard interaction kernel, which represents the quark interchange scattering through the five hard gluon exchanges. These assumption allows to

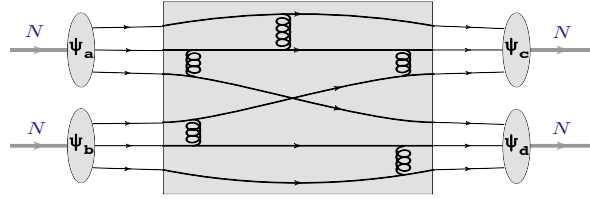


Figure 8. Typical diagram for quark-interchange mechanism of $NN \rightarrow NN$ scattering. represent the amplitude of hard $N(a) + N(b) \rightarrow N(c) + N(d)$ scattering of Fig.8, within quark-interchange approximation in the following form [95]:

$$\begin{aligned} \langle cd | T | ab \rangle &= \sum_{\alpha, \beta, \gamma} \langle \psi_c^\dagger | \alpha'_2, \beta'_1, \gamma'_1 \rangle \langle \psi_d^\dagger | \alpha'_1, \beta'_2, \gamma'_2 \rangle \times \\ &\langle \alpha'_2, \beta'_2, \gamma'_2, \alpha'_1 \beta'_1 \gamma'_1 | H | \alpha_1, \beta_1, \gamma_1, \alpha_2 \beta_2 \gamma_2 \rangle \cdot \langle \alpha_1, \beta_1, \gamma_1 | \psi_a \rangle \langle \alpha_2, \beta_2, \gamma_2 | \psi_b \rangle, \end{aligned} \quad (28)$$

where (α_i, α'_i) , (β_i, β'_i) and (γ_i, γ'_i) describe the spin-flavor quark states of minimal-Fock component of nucleon wave function before and after the hard scattering, H , and

$$C_{\alpha, \beta, \gamma}^j \equiv \langle \alpha, \beta, \gamma | \psi_j \rangle \quad (29)$$

describes the probability amplitude of finding the α, β, γ helicity-flavor combination of three valence quarks in the nucleon j [29, 95]. Note that in Eq.(28) the factorization of nucleon wave functions from the hard scattering kernel is justified by the energies, characteristic to the $C_{\alpha, \beta, \gamma}^j$ factors, being of the order of the nucleon mass, while the H -kernel is characterized by the transferred momenta $-t, -u \gg m_N^2$.

To be able to calculate the $C_{\alpha, \beta, \gamma}^j$ factors, one represents the nucleon wave function through the helicity-flavor basis of the valence quarks. We use a rather general form, separating the nucleon wave function into two parts characterized by two (e.g. second and third) quarks being in spin zero - isosinglet and spin one - isotriplet states as follows:

$$\psi_N^{i^3, h_N} = \frac{1}{\sqrt{2}} \left\{ \Phi_{0,0}(k_1, k_2, k_3) (\chi_{0,0}^{(23)} \chi_{\frac{1}{2}, h_N}^{(1)}) \cdot (\tau_{0,0}^{(23)} \tau_{\frac{1}{2}, i_N^3}^{(1)}) + \Phi_{1,1}(k_1, k_2, k_3) \times \right.$$

$$\sum_{i_{23}^3=-1}^1 \sum_{h_{23}^3=-1}^1 \langle 1, h_{23}; \frac{1}{2}, h_N - h_{23} \mid \frac{1}{2}, h_N \rangle \langle 1, i_{23}^3; \frac{1}{2}, i_N^3 - i_{23}^3 \mid \frac{1}{2}, i_N^3 \rangle \times \\ (\chi_{1,h_{23}}^{(23)} \chi_{\frac{1}{2}, h_N - h_{23}}^{(1)}) \cdot (\tau_{1,i_{23}^3}^{(23)} \tau_{\frac{1}{2}, i_N^3 - i_{23}^3}^{(1)}) \Big\}, \quad (30)$$

where j_N^3 and h_N are the isospin component and the helicity of the nucleon. Here k_i 's are the light cone momenta of quarks which should be understood as $(x_i, k_{i\perp})$, where x_i is a light cone momentum fraction of the nucleon carried by the i -quark. We define $\chi_{j,h}$ and τ_{I,i^3} as helicity and isospin wave functions, where j is the spin, h is the helicity, I is the isospin and i^3 its third component. The Clebsch-Gordan coefficients are defined as $\langle j_1, m_1; j_2, m_2 \mid j, m \rangle$. Here, $\Phi_{I,J}$ represents the momentum dependent part of the wave function for $(I = 0, J = 0)$ and $(I = 1, J = 1)$ two-quark spectator states respectively. We also introduce a parameter, ρ :

$$\rho = \frac{\langle \Phi_{1,1} \rangle}{\langle \Phi_{0,0} \rangle}, \quad (31)$$

which characterizes an average relative magnitude of the wave function components corresponding to $(I = 0, J = 0)$ and $(I = 1, J = 1)$ quantum numbers of two-quark ‘‘spectator’’ states. Note that the two extreme values of ρ define two well known approximations: $\rho = 1$ corresponds to the exact SU(6) symmetric picture of the nucleon wave function and $\rho = 0$ will correspond to the contribution of only good-scalar diquark configuration in the nucleon wave function (see e.g. Ref. [76, 97, 83] where this component is referred to as a scalar or good diquark configuration ($[qq]$) as opposed to a vector or bad diquark configuration denoted by (qq)). In further discussions we will keep ρ as a free parameter. Note that in our approach diquarks represent a qq -component of the nucleon wave function and quarks from the diquark participate in the hard scattering through the quark-interchange.

To calculate the scattering amplitude of Eq.(28) we take into account the conservation of the helicities of quarks participating in the hard scattering. This allows us to approximate the hard scattering part of the amplitude, H , in the following form:

$$H \approx \delta_{\alpha_1 \alpha'_1} \delta_{\alpha_2 \alpha'_2} \delta_{\beta_1 \beta'_1} \delta_{\gamma_1 \gamma'_1} \delta_{\beta_2 \beta'_2} \delta_{\gamma_2 \gamma'_2} \frac{F(\theta)}{s^4}. \quad (32)$$

Inserting this expression into Eq.(28) for the QIM amplitude one obtains [29, 95]:

$$\langle cd \mid T \mid ab \rangle = Tr(M^{ac} M^{bd}) \quad (33)$$

with:

$$M_{\alpha, \alpha'}^{i,j} = C_{\alpha, \beta \gamma}^i C_{\alpha', \beta \gamma}^j + C_{\beta \alpha, \beta}^i C_{\beta \alpha', \beta}^j + C_{\beta \gamma \alpha}^i C_{\beta \gamma \alpha'}^j, \quad (34)$$

where we sum over all the possible values of β and γ .

Furthermore, separating the energy dependence and angular parts for nonvanishing helicity amplitudes of Eq.(2) one obtains:

for $pp \rightarrow pp$:

$$\begin{aligned} \phi_1 &= C(s) [(3+y)F(\theta) + (3+y)F(\pi-\theta)] \\ \phi_3 &= C(s) [(2-y)F(\theta) + (1+2y)F(\pi-\theta)] \\ \phi_4 &= -C(s) [(1+2y)F(\theta) + (2-y)F(\pi-\theta)] \end{aligned} \quad (35)$$

and for $pn \rightarrow pn$:

$$\begin{aligned}\phi_1 &= C(s) [(2-y)F(\theta) + (1+2y)F(\pi-\theta)] \\ \phi_3 &= C(s) [(2+y)F(\theta) + (1+4y)F(\pi-\theta)] \\ \phi_4 &= C(s) [2yF(\theta) + 2yF(\pi-\theta)]\end{aligned}\quad (36)$$

with $\phi_2 = \phi_5 = 0$ due to helicity conservation. Here the function $C(s) = \frac{N}{s^4}$ is due to quark-counting rule with the normalization factor, N , and $F(\theta)$ accounts for the angular dependence generated by hard scattering kernel. In the above equation the parameter:

$$y = x(x+1) \text{ with } x = \frac{2\rho}{3(1+\rho^2)} \quad (37)$$

defines the symmetry of the minimal-Fock (3q) component of nucleon wave function. For example, $\rho = 1$ case reproduces the $SU(6)$ result of Refs. [29] and [30].

As Eqs.(35) and (36) show the helicity amplitudes reveal strong sensitivity to the underlying symmetry of 3q nucleon wave function. The hard kernel, H , as it follows from Eq.(32) defines mainly the overall s -dependence of the amplitudes, thus verifying the dominance of the minimal-Fock component of the quark wave function of nucleon and the QCD mechanism of hard interaction. What concerns the overall normalization of the helicity amplitudes they are defined both by the normalization of the nucleon wave function and the sum of the multitude of hard scattering amplitudes.

In the following we will consider three examples in which the specific measurements can verify the different aspects of the above described model of NN interaction.

Ratio of Differential Cross Sections of Elastic pn and pp Scatterings at $\theta_{cm} = 90^\circ$:

As it can be checked from Eqs.(35) and (36), at $\theta_{cm} = 90^\circ$ the helicity amplitudes of pp scattering depend identically on the helicity-flavor symmetry factor, y of the 3q wave function of the proton, while no such identity exists for pn amplitudes. Therefore one should expect rather strong sensitivity of the ratio of pn to pp elastic cross sections on the underlying spin-flavor symmetry of nucleon wave functions [96]. These can be seen in Fig.9, where the ratio of the differential cross sections of elastic pn to pp scatterings is presented as a function of s at $\theta_{cm} = 90^\circ$. The calculations are performed for the case of $SU(6)$ symmetry ($\rho = 1$) and scalar diquark model, for which $\rho = 0$. The results are compared with the available experimental data. Despite the large errors present in the data, one can clearly see the sensitivity of the considered ratio to the symmetry structure of nucleon wave function with data favoring the scalar diquark model of nucleon.

Angular Asymmetry of Elastic pn Scattering: In this example we demonstrate that an observable such as the asymmetry of a hard elastic proton-neutron scattering with respect to $\theta_{cm} = 90^\circ$ may provide another insight into the helicity-flavor symmetry of the 3q wave function of the nucleon. The measurable quantity we consider is:

$$A_{90^\circ}(\theta) = \frac{\sigma(\theta) - \sigma(\pi - \theta)}{\sigma(\theta) + \sigma(\pi - \theta)}, \quad (38)$$

where $\sigma(\theta)$ is the differential cross section of the elastic pn scattering.

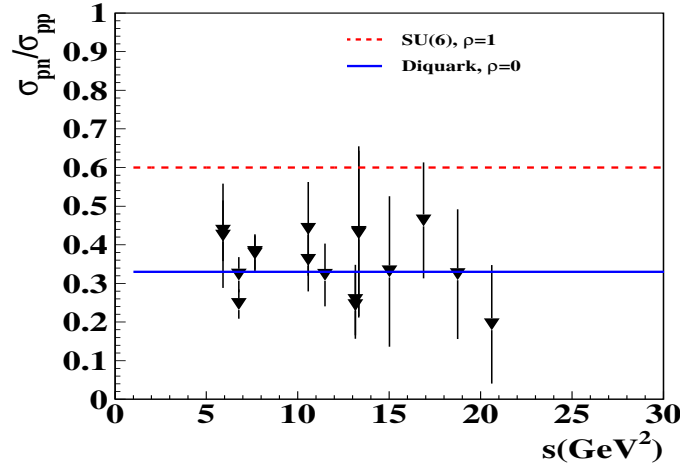


Figure 9. Ratio of the $pn \rightarrow pn$ to $pp \rightarrow pp$ elastic differential cross sections as a function of s at $\theta_{c.m.}^N = 90^\circ$. The data are from Refs. [51, 52, 53, 54].

In Fig.10 the asymmetries of pn scattering calculated with SU(6) ($\rho = 1$) and pure scalar-diquark ($\rho = 0$) models are compared with the data [95]. The comparisons show that the nucleon wave function (30) with the good-scalar diquark component ($\rho = 0$) produces the right sign for the angular asymmetry. On the other the data are in qualitative disagreement with the prediction of exact SU(6) symmetry ($\rho = 1$) of the quark wave function of nucleon.

In Ref. [95] we used ρ as a free parameter to obtain the best fit of the data, which was found for

$$\rho \approx -0.3 \pm 0.2. \quad (39)$$

The nonzero magnitude of ρ indicates the small but finite relative strength of a bad/vector diquark configuration in the nucleon wave function. It is intriguing that the obtained magnitude of ρ is consistent with the 10% probability of “bad” diquark configuration discussed in Ref. [98].

Another interesting property of Eq.(39) is the negative sign of the parameter ρ . Within qualitative quantum-mechanical picture, the negative sign of ρ may indicate for example the existence of a repulsion in the quark-(vector- diquark) channel as opposed to the attraction in the quark - (scalar-diquark) channel. It is rather surprising that both the magnitude and sign agree with the result of the phenomenological interaction derived in the one-gluon exchange quark model discussed in Ref. [97].

The A_{nn} Asymmetry of Elastic pn Scattering: In this last example we consider the $A_{nn} \equiv X_{0,0,n,n}$ asymmetry defined according to Eq.(9). This asymmetry is especially interesting to consider for $\theta_{cm} = 90^\circ$ scattering, since in this case as it was mentioned before the all non-zero helicity amplitudes depend identically on the helicity-flavor factor of y . As a result, by using helicity amplitudes of Eq.(35) in the RHS part of Eq.(9) one

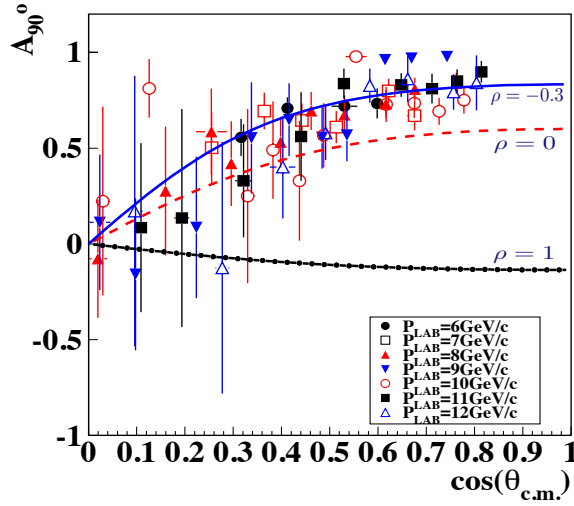


Figure 10. Asymmetry of pn elastic cross section. Solid dotted line - SU(6), with $\rho = 1$, dashed line - diquark model with $\rho = 0$, solid line - fit with $\rho = -0.3$. The data are from Refs. [53, 54].

obtains a constant value, $A_{nn} = 0.333$, at $\theta_{cm} = 90^\circ$ independent on the specific helicity-flavor symmetry of 3q wave functions.

This result is compared with the data in Figs.2 and 4, which demonstrates that agreement with the data happens at $s \approx 18 - 20 \text{ GeV}^2$ at the very same energy range where transparency studies demonstrate the drop of the absorption of propagating "protons" in the nuclear medium (Fig.(3) and (4)).

8. Conclusions and Outlook

In this work we reviewed the current status of QCD studies of hard NN processes that probe quark-gluon interactions at short distances. We gave brief history of these studies and highlighted the outstanding questions that may be resolved in the future experiments at the emerging facilities worldwide. We outlined the theoretical foundation of QCD hard processes and demonstrated that in high energy regime the hard processes probe the minimal (3q) Fock component of the nucleon wave function which is factorized from the kernel that defines the dynamics of the hard scattering.

We considered few examples of application of the outlined approach and demonstrated that even with the limited quantity and quality of the data one can conclude that most probably SU(6) symmetry is breaking down at large x limit of the valence quark component of nucleon wave function. Another observation we made is that, apparently, the phenomenology of hard pp and pn scattering favors the diquark picture of the nucleon with small and finite mixture from the vector diquarks which enter with the negative phase relative to the scalar diquark contribution. Finally, our estimate of the A_{nn} asymmetry of elastic pp scattering within pQCD indicates that it agrees with the data at same energies at which color transparency signature is observed in the hard $A(p, 2p)X$ reactions.

This review covered only the hard elastic NN scatterings. However, it is worth noting that there is a growing activity in studies of NN bound systems at short distances by probing short range correlations in the nuclear wave functions (see e.g. [46, 99, 100, 101, 102]). Currently these studies unambiguously identified the tensor component of short-range NN interactions in the nuclear medium. The planned experiments at the 12 GeV energy upgraded Jefferson Lab [103, 104] will be able to probe the bound NN systems at distances relevant to the nuclear core, where one may expect the onset of QCD degrees of freedom in the similar way as in the hard NN interactions.

Overall new experiments in studies of both hard NN scattering processes and NN short-range correlations in nuclei will provide the necessary ground for advancing the understanding of QCD dynamics of strong forces at short distances.

The author is thankful to Drs. W. Boeglin, S. J. Brodsky, R. Gilman, L. Frankfurt, G. Miller, E. Piasetzky and M. Strikman for illuminating discussions and many years of collaboration on the physics of hard processes. Special thanks to Dr. Igor Strakovsky for the suggestion and opportunity to write this review. This work is supported by the U.S. DOE grant under contract DE-FG02-01ER41172.

References

- [1] E. Rutherford, Phil. Mag. **21**, 669-688 (1911).
- [2] E. Rutherford, Phil. Mag. **37**, 571-580 (1919).
- [3] E. Rutherford, Phil. Mag. **37**, 581-587 (1919).
- [4] John M. Blatt and Victor F. Weisskopf, *Theoretical Nuclear Physics*, Dover Books on Physics, Dover Publications, September, 2010.
- [5] R. Jastrow, Phys. Rev. **81**, 165-170 (1951).
- [6] M. Taketani, S. Nakamura and M. Sasaki, Proc. Theor. Phys. (Kyoto) **6**, 581-586 (1951).
- [7] D. B. Kaplan, M. J. Savage and M. B. Wise, Nucl. Phys. B **534**, 329-355 (1998).
- [8] E. Epelbaum, arXiv:1001.3229 [nucl-th];
- [9] E. Epelbaum, Prog. Part. Nucl. Phys. **57**, 654 (2006).
- [10] C. -J. Yang, C. .Elster and D. R. Phillips, Phys. Rev. C **80**, 044002 (2009).
- [11] R. Machleidt, Adv. Nucl. Phys. **19**, 189 (1989).
- [12] R. B. Wiringa, V. G. J. Stoks and R. Schiavilla, Phys. Rev. C **51**, 38 (1995).
- [13] R. A. Arndt, I. I. Strakovsky and R. L. Workman, Phys. Rev. C **62**, 034005 (2000).
- [14] R. A. Arndt, W. J. Briscoe, I. I. Strakovsky and R. L. Workman, Phys. Rev. C **76**, 025209 (2007).

-
- [15] J. R. Bergervoet, P. C. van Campen, R. A. M. Klomp, J. L. de Kok, T. A. Rijken, V. G. J. Stoks and J. J. de Swart, *Phys. Rev. C* **41**, 1435 (1990).
- [16] R. P. Feynman, “Photon-hadron interactions,” Advanced Book Classics, Addison-Wesley Reading, Massachusetts 282p, 1998.
- [17]
- [18] G. Gaillard, P. Bach, J. Ball, R. Binz, J. Bystricky, P. Demierre, J. M. Fontaine and J. P. Goudour *et al.*, *Helv. Phys. Acta* **64**, 201 (1991).
- [19] S. Kumano, *Nucl. Phys. A* **782**, 442 (2007).
- [20] M. F. M. Lutz *et al.* [PANDA Collaboration], “Physics Performance Report for PANDA: Strong Interaction Studies with Antiprotons,” arXiv:0903.3905 [hep-ex].
- [21] A. N. Sissakian *et al.* [NICA Collaboration], *J. Phys. G* **36**, 064069 (2009).
- [22] J. C. Yang, J. W. Xia, G. Q. Xiao, H. S. Xu, H. W. Zhao, X. H. Zhou, X. W. Ma and Y. He *et al.*, *Nucl. Instrum. Meth. B* **317**, 263 (2013).
- [23] J. F. Gunion, S. J. Brodsky and R. Blankenbecler, *Phys. Rev. D* **8**, 287 (1973).
- [24] D. W. Sivers, S. J. Brodsky and R. Blankenbecler, *Phys. Rept.* **23**, 1 (1976).
- [25] P. V. Landshoff, *Phys. Rev. D* **10**, 1024 (1974).
- [26] V. A. Matveev, R. M. Muradian and A. N. Tavkhelidze, *Lett. Nuovo Cim.* **7**, 719 (1973).
- [27] S. J. Brodsky and G. R. Farrar, *Phys. Rev. Lett.* **31**, 1153 (1973).
- [28] S. J. Brodsky and G. R. Farrar, *Phys. Rev. D* **11**, 1309 (1975).
- [29] G. R. Farrar, S. A. Gottlieb, D. W. Sivers and G. H. Thomas, *Phys. Rev. D* **20**, 202 (1979).
- [30] S. J. Brodsky, C. E. Carlson and H. J. Lipkin, *Phys. Rev. D* **20**, 2278 (1979).
- [31] I. P. Auer, D. Hill, R. C. Miller, K. Nield, B. Sandler, Y. Watanabe, A. Yokosawa and A. Beretvas *et al.*, *Phys. Rev. Lett.* **37**, 1727 (1976).
- [32] I. P. Auer, A. Beretvas, E. Colton, D. Hill, K. Nield, H. Spinka, D. Underwood and Y. Watanabe *et al.*, *Phys. Lett. B* **70**, 475 (1977).
- [33] D. G. Crabb, R. C. Fernow, P. H. Hansen, A. D. Krisch, A. J. Salthouse, B. Sandler, K. M. Terwilliger and J. R. O’Fallon *et al.*, *Phys. Rev. Lett.* **41**, 1257 (1978).
- [34] E. A. Crosbie, L. G. Ratner, P. F. Schultz, J. R. O’Fallon, D. G. Crabb, R. C. Fernow, P. H. Hansen and A. D. Krisch *et al.*, *Phys. Rev. D* **23**, 600 (1981).
- [35] P. Hoyer, arXiv:1402.5005 [hep-ph].

-
- [36] K. Maltman and N. Isgur, Phys. Rev. D **29**, 952 (1984).
- [37] M. Harvey, Nucl. Phys. A **352**, 326 (1981).
- [38] I. T. Obukhovskiy, Y. F. Smirnov and Y. M. Chuvilsky, J. Phys. A **15**, 7 (1982).
- [39] S. J. Brodsky and C. -R. Ji, Phys. Rev. D **33**, 1951 (1986).
- [40] C. -R. Ji and S. J. Brodsky, Phys. Rev. D **34**, 1460 (1986).
- [41] A. M. Kusainov, V. G. Neudatchin and I. T. Obukhovskiy, Phys. Rev. C **44**, 2343 (1991).
- [42] P. Demorest, T. Pennucci, S. Ransom, M. Roberts and J. Hessels, Nature **467**, 1081 (2010).
- [43] H. Heiselberg and V. Pandharipande, Ann. Rev. Nucl. Part. Sci. **50**, 481 (2000).
- [44] E. Piasetzky, M. Sargsian, L. Frankfurt, M. Strikman and J. W. Watson, Phys. Rev. Lett. **97**, 162504 (2006).
- [45] R. Subedi, R. Shneor, P. Monaghan, B. D. Anderson, K. Aniol, J. Annand, J. Arrington and H. Benaoum *et al.*, Science **320**, 1476 (2008).
- [46] L. Frankfurt, M. Sargsian and M. Strikman, Int. J. Mod. Phys. A **23**, 2991 (2008).
- [47] L. Frankfurt and M. Strikman, Int. J. Mod. Phys. E **21**, 1230002 (2012).
- [48] J. P. Ralston and B. Pire, Phys. Rev. Lett. **49**, 1605 (1982).
- [49] S. J. Brodsky and G. F. de Teramond, Phys. Rev. Lett. **60**, 1924 (1988).
- [50] HEPDATA, The Durham HEP database <http://durpdg.dur.ac.uk/hepdata/>.
- [51] J. V. Allaby *et al.*, Phys. Lett. B **28**, 67 (1968).
- [52] C. W. Akerlof *et al.*, Phys. Rev. **159**, 1138 (1967).
- [53] M. L. Perl *et al.*, Phys. Rev. D **1**, 1857 (1970).
- [54] J. L. Stone *et al.*, Nucl. Phys. B **143**, 1 (1978).
- [55] C. Avilez, G. Cocho and M. Moreno, Phys. Rev. D **24**, 634 (1981).
- [56] H. J. Lipkin, Nature **324**, 14 (1986).
- [57] C. Bourrely and J. Soffer, Phys. Rev. D **35**, 145 (1987).
- [58] G. Preparata and J. Soffer, Phys. Lett. B **180**, 281 (1986).
- [59] S. M. Troshin and N. E. Tyurin, JETP Lett. **44**, 149 (1986).
- [60] M. Anselmino, P. Kroll and B. Pire, Z. Phys. C **36**, 89 (1987).

-
- [61] L. E. Gordon and G. P. Ramsey, Phys. Rev. D **59**, 074018 (1999).
- [62] S. J. Brodsky, in *Proceedings of the Thirteenth International Symposium on Multiparticle Dynamics*, edited by W. Kittel, W. Metzger and A. Stergiou, World Scientific, Singapore, p.963 (1981)
- [63] A. H. Mueller, in *Proceedings of the Seventeenth Rencontre de Moriond*, Moriond 1982, edited by J. Tran Thanh Van, Editions Frontiers, Gif-sur-Yvette, France, p.13 (1982).
- [64] L. L. Frankfurt, G. A. Miller and M. Strikman, Ann. Rev. Nucl. Part. Sci. **44**, 501 (1994).
- [65] P. Jain, B. Pire and J. P. Ralston, Phys. Rept. **271**, 67 (1996).
- [66] G. R. Farrar, H. Liu, L. L. Frankfurt and M. I. Strikman, Phys. Rev. Lett. **61**, 686 (1988).
- [67] B. Z. Kopeliovich, J. Nemchik and I. Schmidt, Phys. Rev. C **76** (2007) 015205.
- [68] L. Frankfurt, G. A. Miller and M. Strikman, Phys. Lett. B **304**, 1 (1993).
- [69] L. El Fassi, L. Zana, K. Hafidi, M. Holtrop, B. Mustapha, W. K. Brooks, H. Hakobyan and X. Zheng *et al.*, Phys. Lett. B **712**, 326 (2012).
- [70] B. Clasie, X. Qian, J. Arrington, R. Asaturyan, F. Benmokhtar, W. Boeglin, P. Bosted and A. Bruell *et al.*, Phys. Rev. Lett. **99**, 242502 (2007).
- [71] A. S. Carroll, D. S. Barton, G. Bunce, S. Gushue, Y. I. Makdisi, S. Heppelmann, H. Courant and G. Fang *et al.*, Phys. Rev. Lett. **61**, 1698 (1988).
- [72] I. Mardor, S. Durrant, J. Aclander, J. Alster, D. Barton, G. Bunce, A. Carroll and N. Christensen *et al.*, Phys. Rev. Lett. **81**, 5085 (1998).
- [73] J. Aclander, J. Alster, G. Asryan, Y. Averiche, D. S. Barton, V. Baturin, N. Buktoyarova and G. Bunce *et al.*, Phys. Rev. C **70**, 015208 (2004).
- [74] L. Frankfurt, M. Strikman and M. Zhalov, Phys. Lett. B **503**, 73 (2001).
- [75] L. L. Frankfurt, E. J. Moniz, M. M. Sargsian and M. I. Strikman, Phys. Rev. C **51**, 3435 (1995).
- [76] M. Anselmino, E. Predazzi, S. Ekelin, S. Fredriksson and D. B. Lichtenberg, Rev. Mod. Phys. **65**, 1199 (1993).
- [77] F. Wilczek, In *Shifman, M. (ed.) et al.: From fields to strings, vol. 1* 77-93 [hep-ph/0409168].
- [78] Martin L. Perl, "High Energy Hadrons", John Wiley & Sons Inc , December 4, 1974, 582pp.
- [79] J. Bystricky, F. Lehar and P. Winternitz, J. Phys. (France) **39**, 1 (1978).

-
- [80] N. N. Bogolyubov, V. S. Vladimirov and A. N. Tavkhelidze, *Teor. Mat. Fiz.* **12**, 3 (1972).
- [81] N. N. Bogolyubov, A. N. Tavkhelidze and V. S. Vladimirov, *Teor. Mat. Fiz.* **12**, 305 (1972).
- [82] P. A. M. Dirac, *Rev. Mod. Phys.* **21**, 392 (1949).
- [83] S. Weinberg, *Phys. Rev.* **150**, 1313 (1966).
- [84] S.J. Brodsky, In *Beijing 1993, Proceedings, Particle physics at the Fermi scale* 271-374, and SLAC Stanford - SLAC-PUB-6304 (93/07,rec.Oct.) 104 p
- [85] S. J. Brodsky, H. -C. Pauli and S. S. Pinsky, *Phys. Rept.* **301**, 299 (1998).
- [86] S. J. Brodsky, Lectures at the 58th Scottish University Summer School in Physics: St. Andrews, Schotland, 30 August – 1 September, 2004, hep-ph/0412101.
- [87] G. P. Lepage and S. J. Brodsky, *Phys. Rev. D* **22**, 2157 (1980).
- [88] S. J. Brodsky and J. R. Hiller, *Phys. Rev. C* **28**, 475 (1983) [Erratum-ibid. *C* **30**, 412 (1984)].
- [89] C. White *et al.*, *Phys. Rev. D* **49**, 58 (1994).
- [90] L. L. Frankfurt, G. A. Miller, M. M. Sargsian and M. I. Strikman, *Phys. Rev. Lett.* **84**, 3045 (2000).
- [91] M. M. Sargsian, *Phys. Lett. B* **587**, 41 (2004).
- [92] S. J. Brodsky, L. Frankfurt, R. A. Gilman, J. R. Hiller, G. A. Miller, E. Piasetzky, M. Sargsian and M. Strikman, *Phys. Lett. B* **578**, 69 (2004).
- [93] M. M. Sargsian, *AIP Conf. Proc.* **1056**, 287 (2008).
- [94] M. M. Sargsian and C. Granados, *Phys. Rev. C* **80**, 014612 (2009).
- [95] C. G. Granados and M. M. Sargsian, *Phys. Rev. Lett.* **103**, 212001 (2009).
- [96] C. G. Granados and M. M. Sargsian, *Phys. Rev. C* **83**, 054606 (2011).
- [97] R. L. Jaffe, *Phys. Rept.* **409**, 1 (2005).
- [98] A. Selem and F. Wilczek, in the proceedings of "Ringberg Workshop on New Trends in HERA Physics" 2-7 Oct 2005, Ringberg Castle, Tegernsee, Germany, arXiv:hep-ph/0602128.
- [99] L. L. Frankfurt, M. I. Strikman, D. B. Day and M. Sargsian, *Phys. Rev. C* **48**, 2451 (1993).
- [100] J. Arrington, D. W. Higinbotham, G. Rosner and M. Sargsian, *Prog. Part. Nucl. Phys.* **67**, 898 (2012).

- [101] M. M. Sargsian, Phys. Rev. C **82**, 014612 (2010).
- [102] W. U. Boeglin *et al.* [Hall A Collaboration], Phys. Rev. Lett. **107**, 262501 (2011).
- [103] M. M. Sargsian, J. Arrington, W. Bertozzi, W. Boeglin, C. E. Carlson, D. B. Day, L. L. Frankfurt and K. Egiyan *et al.*, J. Phys. G **29**, R1 (2003).
- [104] White Paper: "The Science Driving the 12 GeV Upgrade of CEBAF", Jefferson Lab, Newport News, VA, 2000.